Fentanyl-related designer drugs W-18 and W-15 lack appreciable opioid activity in vitro and in vivo

Xi-Ping Huang,[1,2] Tao Che,[1] Thomas J. Mangano,[1,2] Valerie Le Rouzic,[3] Ying-Xian Pan,[3] Susruta Majumdar,[3] Michael D. Cameron,[4] Michael H. Baumann,[5] Gavril W. Pasternak,[3] and Bryan L. Roth[1,2]

[1]Department of Pharmacology, University of North Carolina School of Medicine, Chapel Hill, North Carolina, USA. [2]National Institute of Mental Health Psychoactive Drug Screening Program, Chapel Hill, North Carolina, USA. [3]Department of Neurology and Molecular Pharmacology Program, Memorial Sloan Kettering Cancer Center, New York, New York, USA. [4]Department of Molecular Therapeutics, The Scripps Research Institute, Jupiter, Florida, USA. [5]Designer Drug Research Unit, Intramural Research Program, National Institute on Drug Abuse, National Institutes of Health, Baltimore, Maryland, USA.

W-18 (4-chloro-N-[1-[2-(4-nitrophenyl)ethyl]-2-piperidinylidene]-benzenesulfonamide) and W-15 (4-chloro-N-[1-(2-phenylethyl)-2-piperidinylidene]-benzenesulfonamide) represent two emerging drugs of abuse chemically related to the potent opioid agonist fentanyl (N-(1-(2-phenylethyl)-4-piperidinyl)-N-phenylpropanamide). Here, we describe the comprehensive pharmacological profiles of W-18 and W-15, as examination of their structural features predicted that they might lack opioid activity. We found W-18 and W-15 to be without detectible activity at μ, δ, κ, and nociception opioid receptors in a variety of assays. We also tested W-18 and W-15 for activity as allosteric modulators at opioid receptors and found them devoid of significant positive or negative allosteric modulatory activity. Comprehensive profiling at essentially all the druggable GPCRs in the human genome using the PRESTO-Tango platform revealed no significant activity. Weak activity at the sigma receptors and the peripheral benzodiazepine receptor was found for W-18 (K_i = 271 nM). W-18 showed no activity in either the radiant heat tail-flick or the writhing assays and also did not induce classical opioid behaviors. W-18 is extensively metabolized, but its metabolites also lack opioid activity. Thus, although W-18 and W-15 have been suggested to be potent opioid agonists, our results reveal no significant activity at these or other known targets for psychoactive drugs.

Introduction

W-18 (4-chloro-N-[1-[2-(4-nitrophenyl)ethyl]-2-piperidinylidene]-benzenesulfonamide) and W-15 (4-chloro-N-[1-(2-phenylethyl)-2-piperidinylidene]-benzenesulfonamide) were originally identified in the patent literature as analogs of the potent opioid agonist fentanyl (N-(1-(2-phenylethyl)-4-piperidinyl)-N-phenylpropanamide) (Figure 1) (1). Given the fact that W-18 and W-15 differ in key respects chemically from fentanyl (Figure 1), it could be predicted that they might lack appreciable opioid receptor agonist actions. The presence of an aryl sulfonamide group renders the piperidine nitrogen atom nonbasic. A basic tertiary amine is commonly seen in most opioid templates. It could thereby be predicted that both W-15 and W-18 might lack appreciable opioid receptor agonist activity. In the original description, W-18 and W-15 (along with several other analogs) were described to be extraordinarily potent at inhibiting phenylquinone-induced writhing — a mouse model useful for assessing potential analgesic actions for a wide variety of drugs, such as aspirin, antihistamines, opioids, antidepressants, sympathomimetics, acetylcholinesterase inhibitors, and psychotomimetic opioids, such as cyclazocine (2). Thus, the inhibition of phenylquinone-induced writhing is a relatively nonspecific test for drugs with potential analgesic and other activities. In the original report, there was no evidence that the activity in this model by either W-18 or W-15 was antagonized by the prototypical opioid antagonist naloxone, although the related compound W-20 (1-cyclopropylmethylpiperidylidene-2-(4-chlorophenyl)sulfonamide) was reported to have modest naloxone-reversible activity.

Conflict of interest: The authors have declared that no conflict of interest exists.

Submitted: August 31, 2017
Accepted: October 17, 2017
Published: November 16, 2017

Reference information:
JCI Insight. 2017;2(22):e97222.
https://doi.org/10.1172/jci.insight.97222.

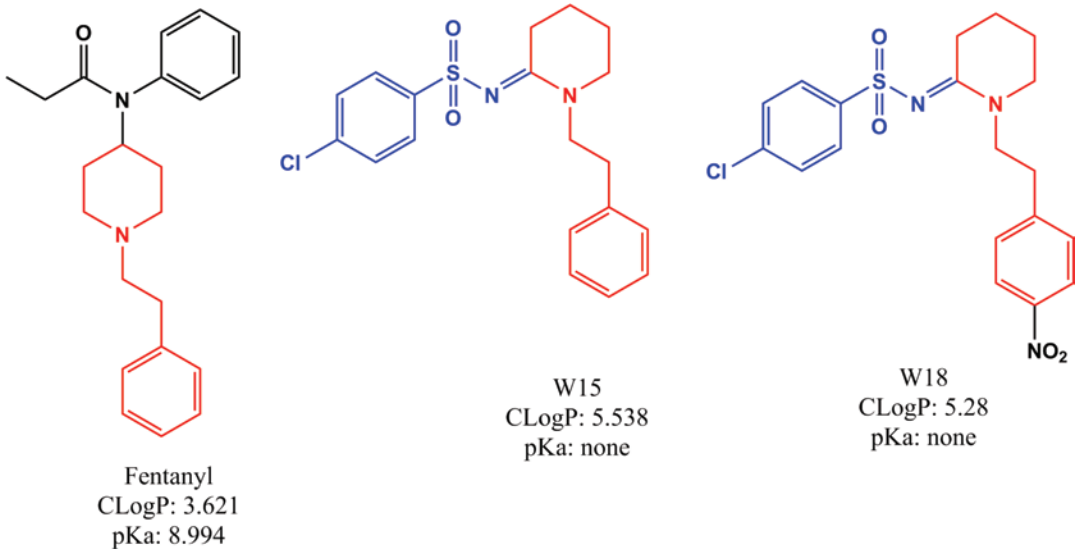

Figure 1. Structure of fentanyl, W-15, and W-18. Shown are the chemical structures of fentanyl (left), W-15 (center), and W-18 (right). The structural similarities between fentanyl and W-15/W-18 are shown in red. The presence of aryl sulfonamide group (in blue) in both W-15/W-18 makes the piperidine nitrogen not charged at physiological pH compared with the fentanyl piperidine nitrogen.

Recently, W-18 (3–7) and perhaps W-15 have emerged as potential drugs of abuse; W-18 is scheduled as a controlled substance in Canada (8) and is being considered for inclusion in Schedule 1 control in the US. To our knowledge, there are no other published reports on the pharmacology of W-18 or W-15. Accordingly, we here report a comprehensive evaluation of the in vitro molecular pharmacology of W-18 and W-15.

Results

Radioligand-binding assays reveal no activity of W-18 at human, cloned opioid receptors. In our initial studies, we evaluated the ability of W-15 and W-18 to interact with 3 canonical opioid receptors via radioligand-binding studies performed as previously described using cloned, human κ (9, 10), μ (11), and δ opioid receptors (KOR, MOR, and DOR, respectively) (12, 13). No significant inhibition of radioligand binding was measured up to concentrations as high as 10,000 nM (Table 1). These studies were followed by investigation of effects against the murine MOR, KOR, and DOR, with similar results. No inhibition of binding with concentrations as high as 1 μM were observed. W-15 and/or W-18 inhibited radioligand binding at several nonopioid receptors with low affinities, including the 5-HT_{2A}, 5-HT_{2B}, 5-HT_{2C}, and 5-HT_6 serotonin receptors; benzodiazepine receptors (BZP and PBR) (Table 1); and other miscellaneous targets (Table 2).

Functional assays reveal no agonist, antagonist, or allosteric modulator activity of W-18 or W-15 at human cloned opioid receptors. We next evaluated W-18 and W-15 for agonist and antagonist activity at cloned human opioid receptors in both G_i-dependent inhibition of cAMP production and G protein–independent arrestin translocation assays (Figures 2 and 3). No significant agonist or antagonist activity was measured up to doses as high as 10,000 nM, although nonspecific agonist effects were evident at high concentrations in these assays (Figure 2, A–D). We also evaluated the potential of W-18 to be an allosteric modulator of opioid receptors and found only weak and potentially nonspecific negative allosteric modulator actions in either G_i-cAMP or arrestin signaling (Figures 4 and 5).

Functional assays reveal antagonist activity at human 5-HT receptors. Since W-15 and W-18 displayed binding activities at 5-HT_2 and 5-HT_6 receptors, we examined their functional activity at 5-HT_{2A}, 5-HT_{2B}, and 5-HT_{2C} receptors for calcium mobilization and at 5-HT_6 receptors for arrestin signaling. W-15 and W-18 showed no agonist activity and modest antagonist activity at 5-HT_2 receptors (Figure 6). Schild analysis with W-15 indicated competitive antagonism against 5-HT at 5-HT_2 receptors, as shown by the parallel shifts of the agonist dose-response curves (Figure 7). At 5-HT_6 receptors, W-15 and W-18 displayed no agonist activity (Figure 8). W-15 and W-18 also displayed weak binding at

Table 1. W-15 and W-18 binding profiles

Receptor	Inhibition (%)	
	W-15	W-18
5-HT_{1A}	25.0	–6.6
5-HT_{1B}	–6.6	–1.6
5-HT_{1D}	17.6	12.3
5-HT_{1E}	–7.5	–18.9
5-HT_{2A}	96.5	50.9
5-HT_{2B}	87.3	60.8
5-HT_{2C}	95.7	80.1
5-HT_{3}	3.1	14.2
5-HT_{5A}	–9.5	3.2
5-HT_{6}	88.1	69.1
5-HT_{7}	27.2	–7.3
A_1	65.8	49.9
A_{2A}	54.6	43.3
α_{1A}	–2.8	17.3
α_{1B}	–13.7	–3.7
α_{1D}	3.9	–2.8
α_{2A}	83.5	66.5
α_{2B}	3.0	7.5
α_{2C}	20.2	–14.8
β_1	–9.8	1.3
β_2	–6.4	–8.0
β_3	23.4	9.8
BZP	84.0	72.8
CB_1	ND	ND
CB_2	34.1	31.4
D_1	18.0	4.1
D_2	–5.9	0.3
D_3	–12.3	3.0
D_4	–3.9	1.8
D_5	26.3	4.6
DAT	21.0	6.7
NET	50.8	16.3
SERT	38.4	18.5
DOR	34.8	–4.5
KOR	30.3	–5.4
MOR	33.0	14.8
GABAA	20.0	18.3
hERG	72.4	71.4
H_1	27.6	1.4
H_2	24.5	27.3
H_3	4.5	3.2
H_4	40.5	1.7
M_1	25.5	18.1
M_2	14.7	–14.0
M_3	12.8	14.4
M_4	27.3	6.8
M_5	21.8	12.5
$mGluR_5$	38.9	46.8
PBR	96.8	95.9
Sigma 1	23.9	13.9
Sigma 2	35.0	48.8
V_{1A}	65.1	64.2
V_{1B}	30.5	33.4
V_2	36.2	28.2
OT	17.8	2.2

Results represent mean percentage of inhibition at 10 μM. Values are averages from triplicate or quadruplicate sets. BZP, brain benzodiazepine binding site (rat); PBR, peripheral benzodiazepine receptors; ND, not determined.

Table 2. Binding affinities of W-15 and W-18 for targets with >50% inhibition in initial screen

Receptor	K_i (pK_i ± SEM, *n*)	
	W-15	W-18
5-HT_{2A}	109 nM (6.96 ± 0.05, 3)	1,751 nM (5.76 ± 0.20, 3)
5-HT_{2B}	380 nM (6.42 ± 0.11, 3)	2,171 nM (5.66 ± 0.19, 3)
5-HT_{2C}	52 nM (6.91 ± 0.07, 3)	878 nM (6.06 ± 0.05, 3)
5-HT_6	123 nM (6.91 ± 0.09, 3)	1,008 nM (6.00 ± 0.05, 3)
BZP	933 nM (6.03 ± 0.06, 3)	1,023 nM (5.99 ± 0.55, 3)
PBR	70 nM (7.16 ± 0.27, 4)	77 nM (7.11 ± 0.24, 4)
A_1	3,846 nM (5.42 ± 0.05, 2)	5,129 nM (5.29 ± 0.07, 2)
α_{2A}	2,818 nM (5.55 ± 0.23, 4)	2,138 nM (5.67 ± 0.20, 4)
CB_2	8,511 nM (5.07 ± 0.06, 3)	7,470 nM (5.13 ± 0.08, 3)
V_{1a}	3,575 nM (5.45 ± 0.12, 3)	3,311 nM (5.48 ± 0.19, 3)
hERG	2,042 nM (5.69 ± 0.09, 3)	1,806 nM (5.74 ± 0.07, 3)

pK_i represents the -log of the Ki value

A_1-adenosine, α_{2A}-adrenergic, and CB_2 cannabinoid receptors; we therefore examined the nature of their activity at these receptors. Our results (Figure 8) indicated that the drugs had no agonist activity at any of these examined receptors.

Screening of W-18 and W-15 against the druggable GPCR-ome revealed no significant agonist activity at any human druggable GPCR. We next screened W-18 and W-15 against the druggable human GPCR-ome using our recently developed PRESTO-Tango resource (14). Although no significant agonist activity was reproducibly found, we did note that concentrations of W-18 higher than 1 μM tended to cause a decrease in the overall baseline activity for nearly every target, consistent with a toxic activity at HEK cells with prolonged incubation (Figure 9).

We examined the metabolism of W-18. W-18 was extensively metabolized by both human and mouse liver microsomes (Supplemental Figures 1–3), resulting in multiple monohydroxylated and dihydroxylated metabolites as well as a dealkylated and an amino metabolite from reduction of the nitro group. To determine if W-18 was a prodrug, releasing an active compound through metabolism, we incubated W-18 with liver microsomes, extracted the remaining W-18 and its metabolites, and tested the mixture in opioid receptor–binding assays at a concentration corresponding to 1 μM W-18 prior to the microsomal incubation. The mixture of W-18 and metabolites failed to significantly inhibit binding to murine MOR, DOR, or KOR expressed in Chinese hamster ovary (CHO) cells.

In silico studies. We also used the similarity ensemble approach to determine if any molecular targets might be predicted with high expectancies to have activity for W-18. No target(s) emerged with high confidence, although weak predictions ($E = 4.67\ e^{-1}$) suggested activity were for H_3-histamine for W-18, which was not confirmed experimentally (Table 1).

In vivo evaluation. In the initial patent report, W-18 was active in the writhing assay, with a potency many times that of morphine. When administered in mice at doses as high as 1 mg/kg, s.c., W-18 failed to demonstrate any activity in either the radiant heat tail-flick assay or the writhing assay (Figure 10 and Table 3). Treated mice failed to display classical opioid behaviors, such as hyperlocomotion or Straub tail (Table 3). A general behavioral action of burrowing into the bedding was observed that is not associated with classical opioids, and the animals were clearly atypical in their overall behavior, showing a general tunneling behavior. Administration of naloxone failed to counteract these behaviors. Similar burrowing behaviors were seen in rats after s.c. administration of 0.3 and 1.0 mg/kg.

Discussion

The major findings of these studies are that both W-18 and W-15 are devoid of significant opioid receptor activity. Although W-18 and W-15 were described in the initial patent report as having potent analgesic activity in the phenylquinone-induced writhing assay, it should be noted that the test used cannot definitively identify the molecular target for the presumed "analgesic activity." The nociceptive stimulus is relatively weak, with opioids active at doses far below those needed in thermal assays. Thus, as originally reported (2),

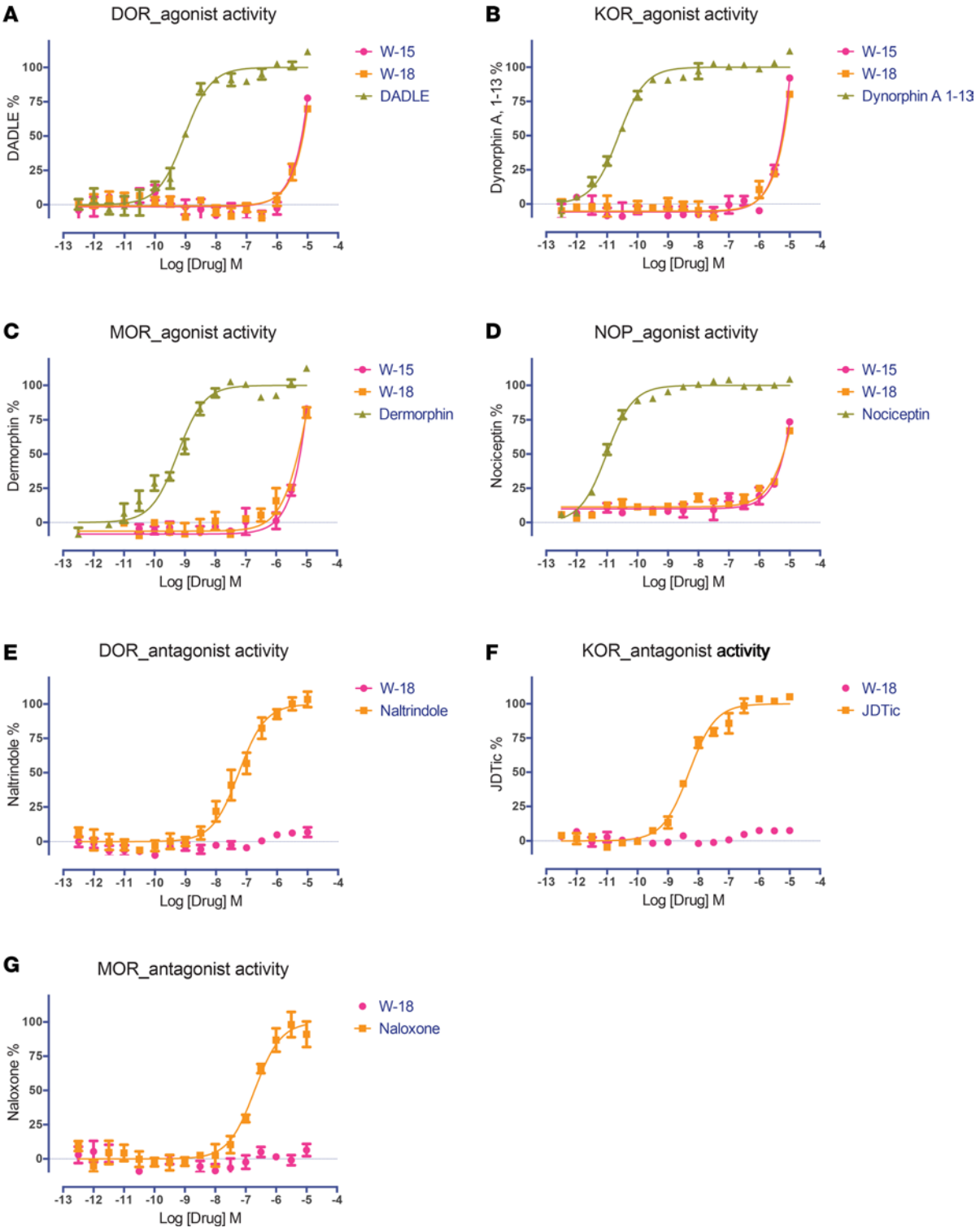

Figure 2. Effect of W-15 and W-18 on opioid receptor–mediated $G_{\alpha i}$ signaling. The G_i-mediated inhibition of cAMP production was determined as previously described (9–11). Both W-15 and W-18 showed no agonist activity at DOR (**A**), KOR (**B**), MOR (**C**), and nociceptin (NOP) (**D**) receptors and no antagonist activity at DOR (**E**), KOR (**F**), or MOR (**G**) receptors. Normalized results represent mean ± SEM of 3 independent experiments, each performed in triplicate (0% activity for vehicle activity; 100% for reference activity), and were analyzed in Prism.

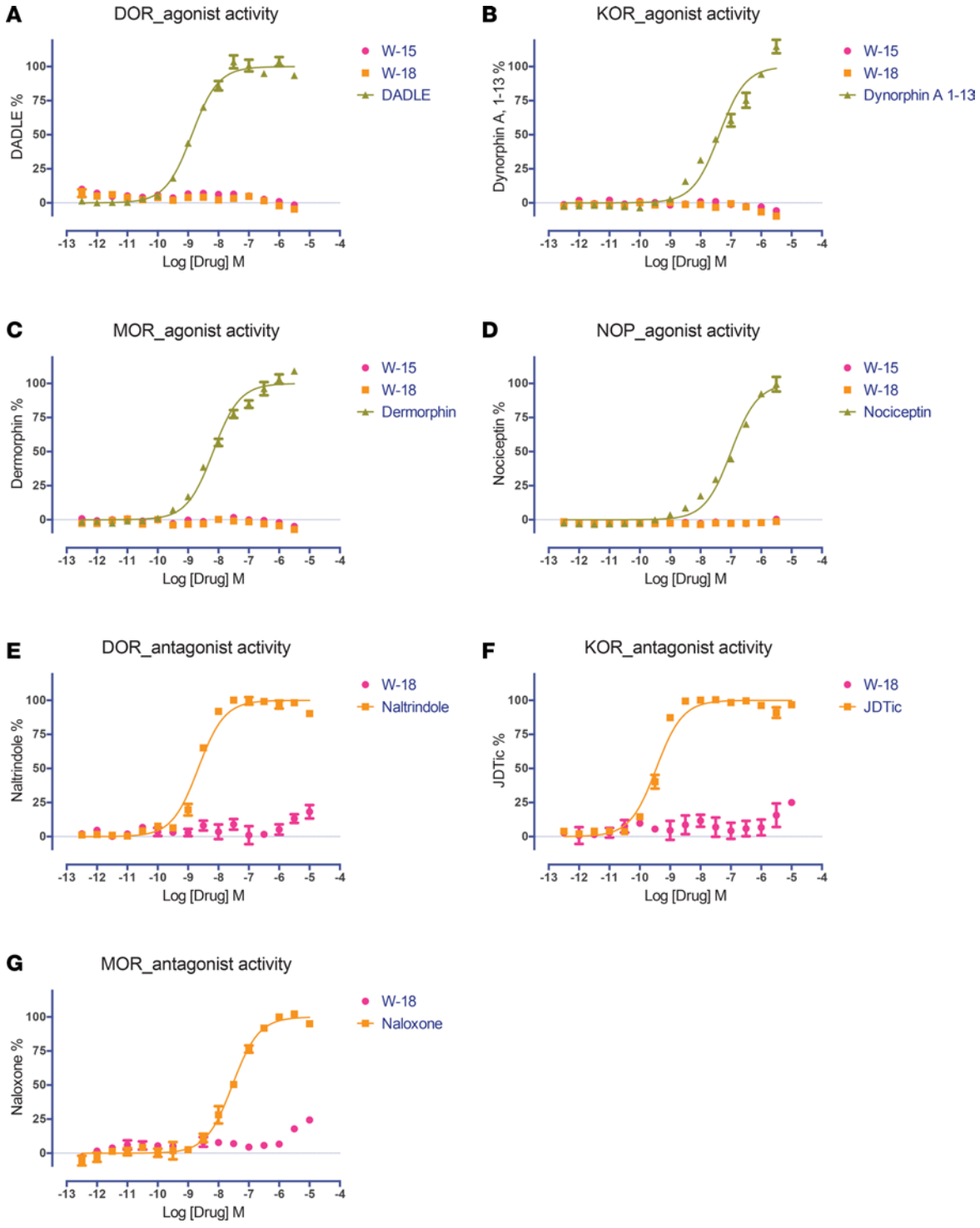

Figure 3. Effect of W-15 and W-18 on opioid receptor–mediated β-arrestin recruitment. G protein–independent arrestin recruitment was determined in the GPCR Tango assay, as outlined in the Methods. Both W-15 and W-18 were tested and showed no agonist activity at DOR (**A**), KOR (**B**), MOR (**C**), and NOP (**D**) receptors and no antagonist effect at DOR (**E**), KOR (**F**), or MOR (**G**) receptors. Normalized results represent mean ± SEM of 3 independent experiments, each performed in triplicate (0% for vehicle activity, and 100% for reference activity), and were analyzed in Prism.

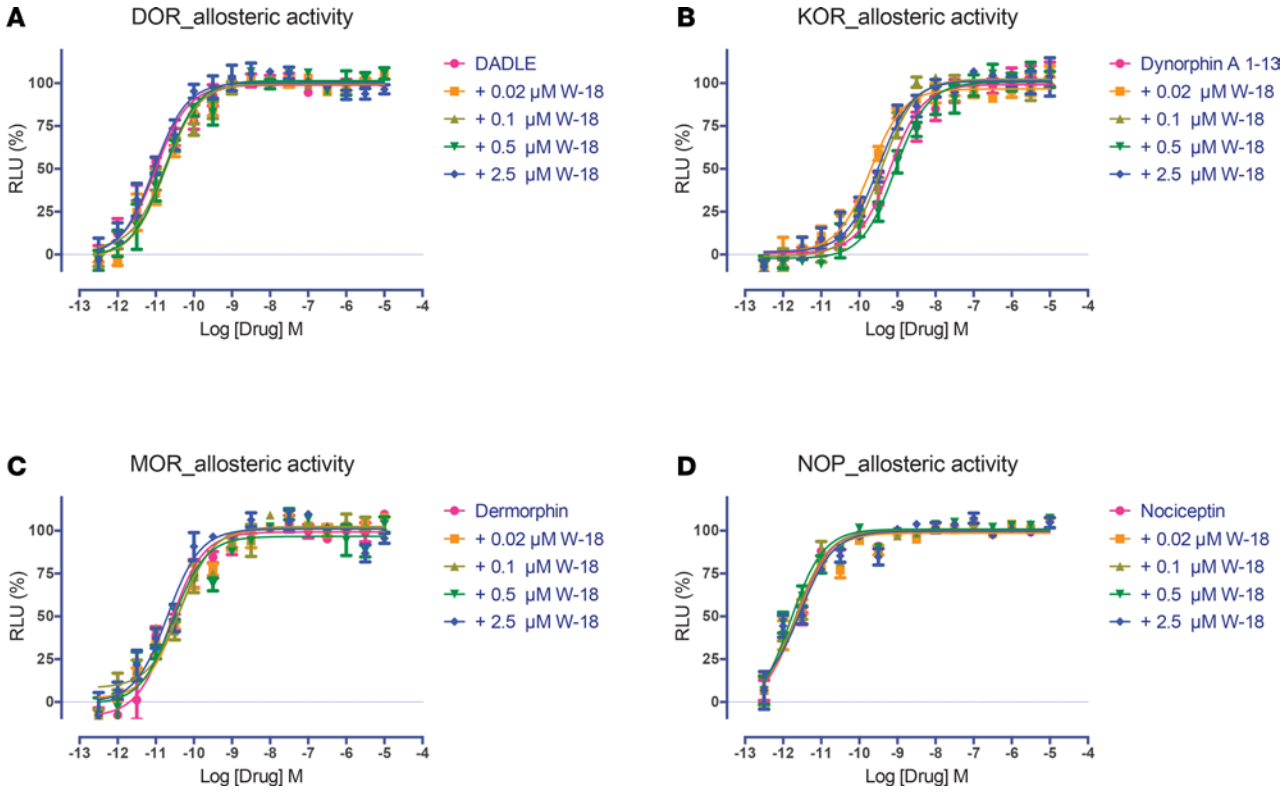

Figure 4. Allosteric activity of W-18 on agonist stimulated inhibition of cAMP accumulation at opioid receptors. The G_i-mediated inhibition of cAMP production was determined as previously described (9–11) and in Methods. W-18 failed to modify the effect of DADLE at DOR (**A**), dynorphin A at KOR (**B**), dermorphin at MOR (**C**), or nociceptin at NOP (**D**) receptors. Normalized results represent mean ± SEM of 3 independent experiments, each performed in triplicate (0% for vehicle activity and 100% for reference activity), and were analyzed in Prism.

a large assortment of pharmacological agents show activity in this assay, including cholinesterase inhibitors, antihistamines, and antidepressants (15). In our hands, W-18 revealed no antinociceptive activity in either the thermal radiant heat tail-flick assay or the writhing assay. Furthermore, the atypical behaviors observed with the drugs (i.e., tunneling) failed to be reversed by naloxone, indicating that opioid receptors are not involved.

It is conceivable that W-18 and W-15 are prodrugs that require metabolic transformation for their effects in humans, as has been seen for toxic pharmaceuticals, including fenfluramine (16) and methysergide (17). Even the prescribed analgesic codeine requires demethylation to generate morphine for activity in both receptor-binding assays and in vivo. W-18 undergoes extensive metabolism in both human and mouse liver microsomes; however, these metabolites do not reveal any affinity for opioid receptors. Behaviorally, W-18 failed to elicit any naloxone-sensitive actions. In addition, we saw no inhibition of murine opioid receptor–binding from the W-18 metabolite mixture. The hepatic microsomal incubations provide an assessment of in vivo relevant metabolites but may not be comprehensive with respect to conjugation reactions, such as glucuronidation of primary W-18 metabolites. Although further studies aimed at identifying the individual metabolite(s) and determining their pharmacological activities are needed, and may uncover mechanisms contributing to the abuse potential of W-18, our studies strongly indicate that opioid systems are not involved.

In conclusion, comprehensive evaluation of the potential in vitro molecular pharmacology of W-18 and W-15 revealed no consensus targets for interaction. Although apparently devoid of opioid receptor activity, weak activity of W-18 at the peripheral benzodiazepine receptor was found, and the drugs appear to exhibit toxicity in HEK cells with overnight incubation at concentrations higher than 1 μM. The literature has suggested that W-18 falls into the opioid class of drugs, possibly providing a false sense of security for those abusing the compound who may rely upon its reversibility by naloxone. Given the lack of apparent activity at human or mouse cloned opioid receptors for the parent compounds or the metabolites, the utility of naloxone and other opioid antagonists in treating overdose in humans is unlikely to be successful. This needs to be understood by both first responders and those abusing the compound.

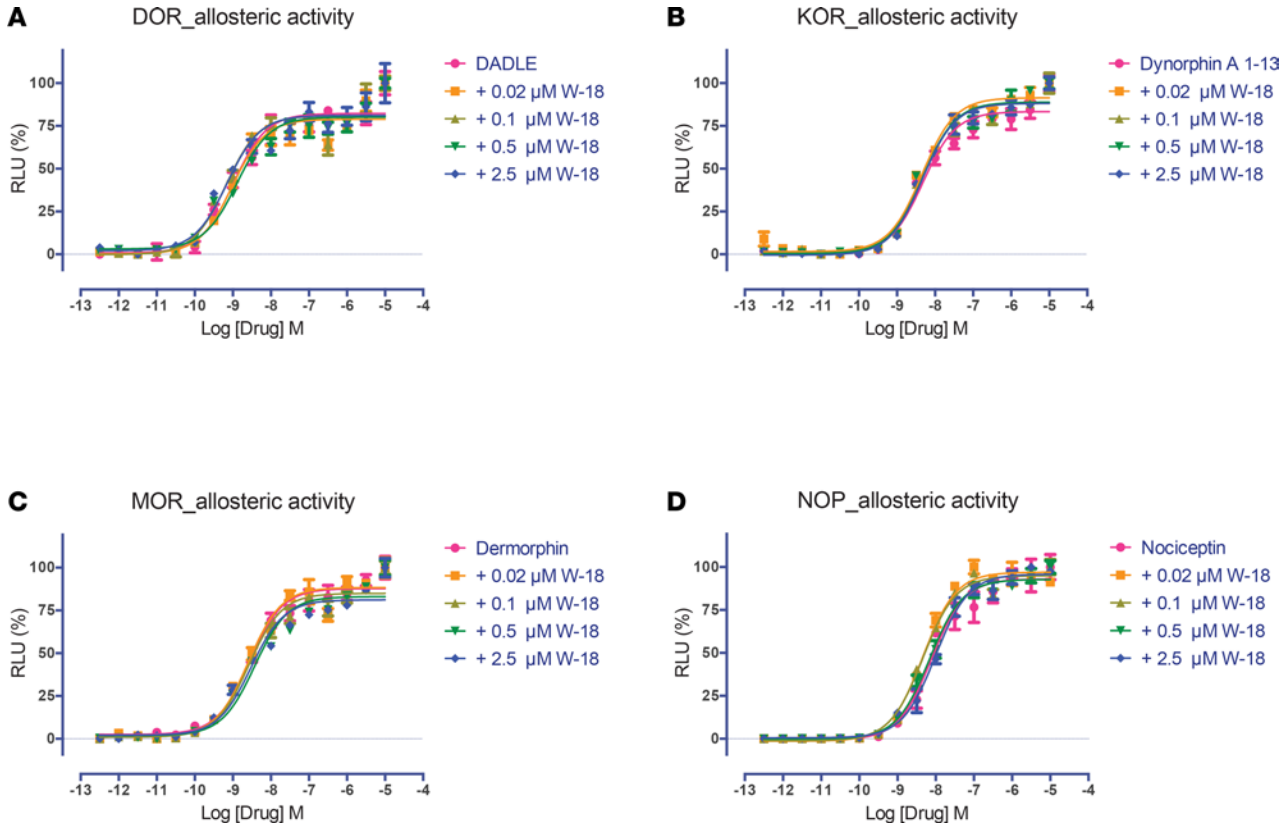

Figure 5. Allosteric activity of W-18 on agonist stimulated β-arrestin recruitment at opioid receptors. The arrestin recruitment activity was determined in the GPCR Tango assays, as outlined in the Methods. W-18 failed to modify the effect of DADLE at DOR (**A**), dynorphin A at KOR (**B**), dermorphin at MOR (**C**), or nociceptin at NOP (**D**) receptors. Normalized results represent mean ± SEM of 3 independent experiments, each performed in triplicate (0% activity for vehicle and 100% for reference activity), and were analyzed in Prism.

Methods

Drugs. W-18 and W-15 were purchased from Cayman Chemicals and supplied as >98% pure. Independent LC-MS quality control revealed the compounds were both pure and authentic.

Mice. CD-1 mice (20–30 g) were obtained from Charles River Laboratories and maintained on normal chow.

Cell lines. HEK93T cells were obtained from ATCC (catalog CRL-3216), and HTLA cells were obtained from Richard Axel (Columbia University).

Radioligand-binding assays. Radioligand-binding studies were performed as previously described using cloned, human receptors (18). Comprehensive profiling was performed using the resources of the National Institute of Mental Health Psychoactive Drug Screening Program as described previously (18). Initial screens were performed at 10,000 nM in quadruplicate. For targets with inhibition >50%, we also carried out concentration-response binding assays to determine affinities (K_i). Follow-up assays on murine opioid receptors expressed in CHO cells were carried out as previously described (19).

Metabolism studies. Metabolism was assessed using both mouse liver microsomes and pooled human liver microsomes incubated with NADPH (1 mM). Heat-inactivated microsomes and incubations without NADPH were used as controls. At various time points, 2 times the volume of acetonitrile was added to stop the incubation and precipitate the protein so the sample could be analyzed by mass spectrometry. Samples were analyzed using multiple methods on a Sciex 6500, operating in multiple reaction monitoring mode using predicted mass transitions, using precursor ion and product ion scans. Samples were further analyzed on a Thermo Scientific Q Exactive high-resolution mass spectrometer using full-scan mode operating at 70,000 resolution. Samples were also evaluated by HPLC using UV detection. HPLC-UV samples were processed by solid-phase extraction, dried using a vacuum centrifuge and reconstituted in a minimal volume of mobile phase.

In addition, a W-18 mixed-metabolite sample was prepared by incubating 40 μl of a 20 mM W-18 DMSO stock with 5 ml of 1 mg/ml human liver microsomes or mouse liver microsomes and 1 mM

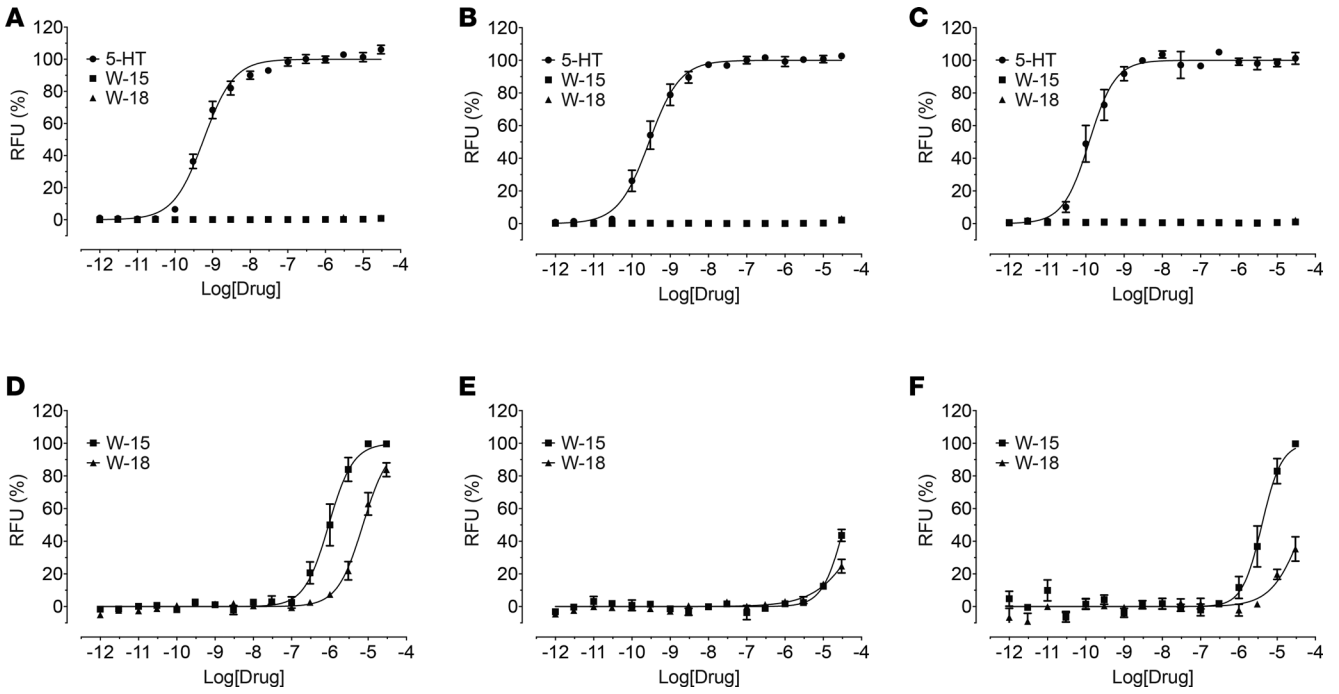

Figure 6. Agonist activities and antagonist effects of W-15 and W-18 at 5-HT$_{2A}$, 5-HT$_{2B}$, and 5-HT$_{2C}$ receptors. G_q-mediated calcium mobilization activity was determined using HEK293 cells stably expressing corresponding 5-HT$_2$ subtypes on FLIPR^{TETRA}. Normalized results (relative fluorescence unit in fold of basal, basal was set as 0% and 5-HT E_{max} was set as 100%) represented mean values ± SEM from 2 independent assays, each performed in quadruplicate, and were analyzed in Prism. In antagonist activity assays, the reference agonist (5-HT) was used at a final concentration of 10 nM and was set as 0% inhibition and basal was set as 100% inhibition. Panels **A–C** represent dose-response curves to 5-HT, W-15 and W-18 at 5-HT2A (**A**), 5-HT2B (**B**), or 5-HT2C (**C**) receptors. Panels **D–F** shows the antagonist activity of W-15 and W-18 at 5-HT2A (**D**), 5-HT2B (**E**), or 5-HT2C (**F**) receptors.

NADPH for 90 minutes. Metabolites were isolated using solid-phase extraction and dried using a speed vacuum. The mixed-metabolite sample was resolubilized, and the pooled metabolites were examined in opioid receptor–binding assays using the murine receptors expressed in CHO cells at concentrations corresponding to an initial concentration of W-18 an initial concentration of W-18 of 1 μM.

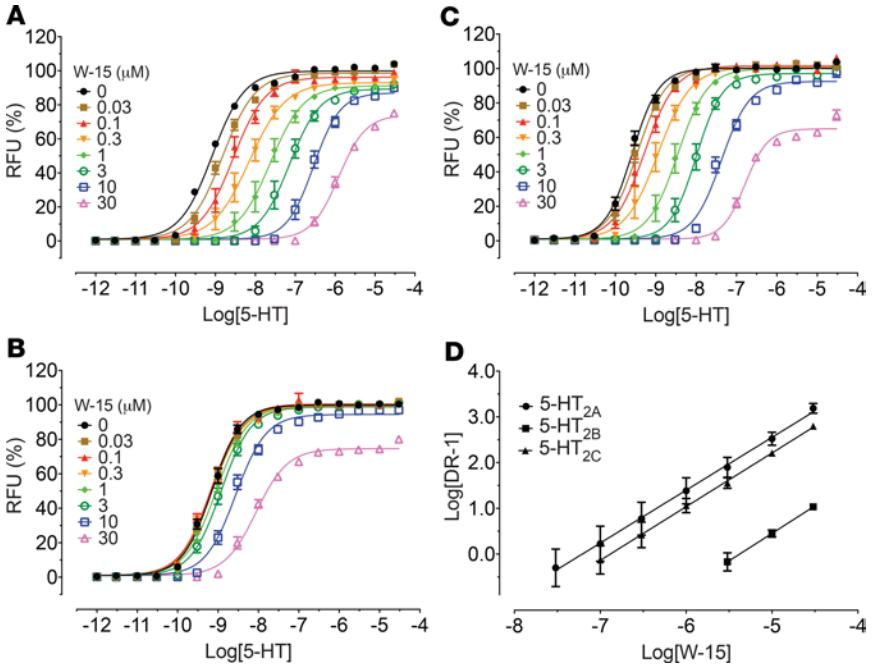

Figure 7. Concentration-dependent effect of W-15 on 5-HT activity at 5-HT$_{2A}$, 5-HT$_{2B}$, and 5-HT$_{2C}$ receptors. 5-HT–mediated calcium mobilization was determined in the absence and presence of increasing concentrations of W-15 using HEK293 cells stably expressing corresponding 5-HT$_2$ subtypes on FLIPR-^{TETRA}. Normalized results (relative fluorescence unit in fold of basal, basal was set as 0%, and 5-HT E_{max} in the absence of W-15 was set as 100%) represented mean values ± SEM from 3 independent assays, each performed in triplicate, and were analyzed in Prism. Schild plot analysis (**D**) indicated W-15 is a competitive antagonist against 5-HT. The average pA_2 values are 7.20 (5-HT$_{2A}$), 5.38 (5-HT$_{2B}$), and 6.88 (5-HT$_{2C}$). Panels **A–C** represent oncentration response curves for W-15 with increasing concentrations of 5-HT at 5-HT2A (**A**), 5-HT2B (**B**), or 5-HT2C (**C**) receptors.

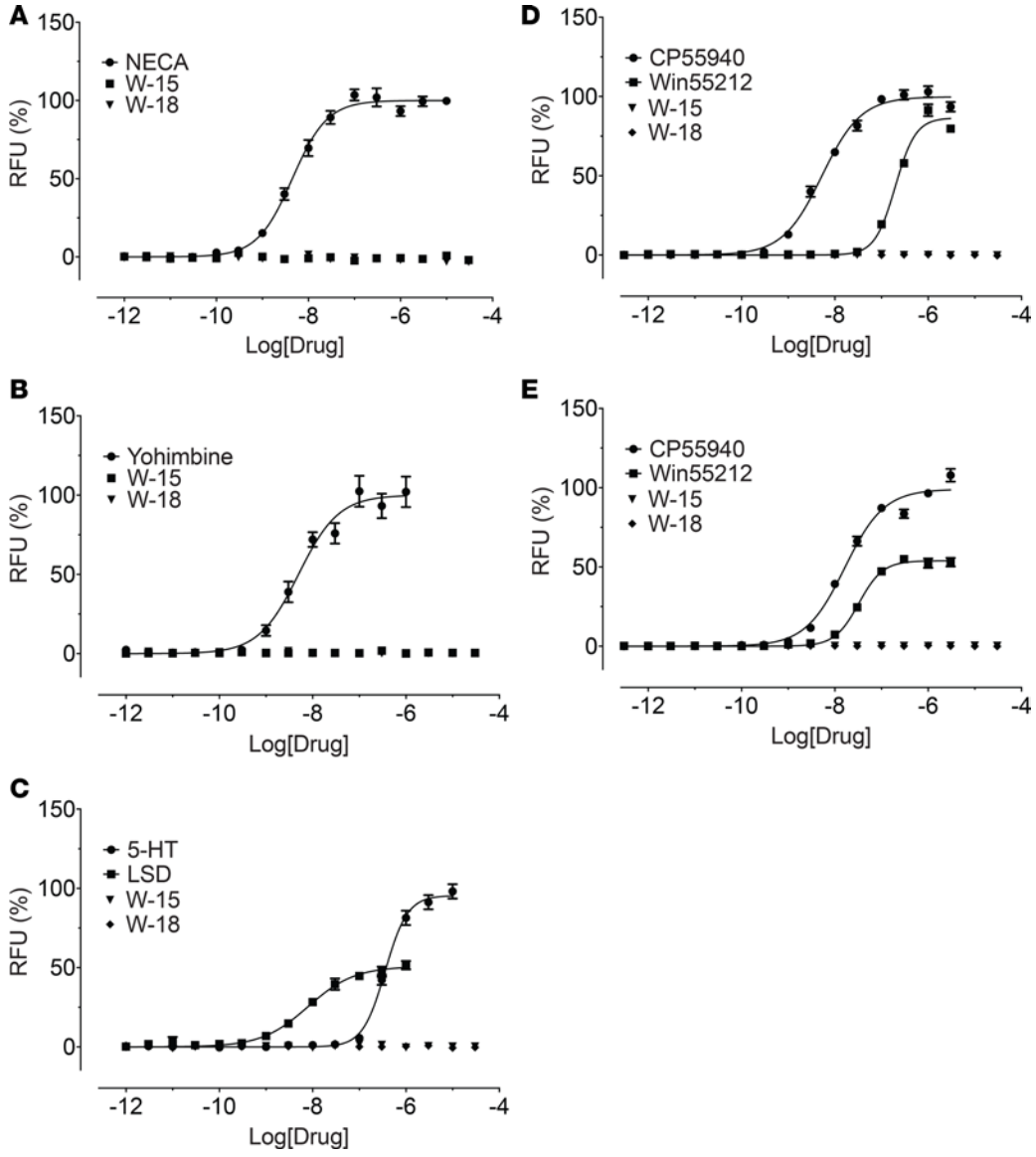

Figure 8. W-15 and W-18 have no agonist activity at A_1, α_{2A}, 5-HT_6, CB_1, or CB_2 receptors. Agonist activity (arrestin recruitment) was determined in GPCR Tango assays, as outlined in the Methods. Normalized results (basal was set as 0% and reference E_{max} was set as 100%) represented mean ± SEM from minimum of *n* assays (*n* = 2 for **A** and **B**, *n* = 3 for **C–E**), each performed in triplicate, and were analyzed in Prism. Panels **A–E** represent a dose response curve for A1-adenosine (**A**), a2-adrenergic (**B**), 5-HT6 receptors (**C**), CB1 receptors (**D**), or CB2 receptors (**E**).

Opioid receptor functional assays. Assays for agonist and antagonist activity at cloned opioid receptors were performed as previously described using cloned, human κ (9, 10), μ (11), δ, and nociceptin opioid receptors (12, 13). Assays for evaluating the allosteric modulation of opioid receptors were performed using graded concentrations of potential allosteric modulators in the absence and presence of increasing concentrations of the orthosteric ligand in a manner similar to a manner we recently described (20).

Profiling of W-18 and W-15 against the druggable GPCR-ome. These studies were performed using our recently described PRESTO-Tango resource (14), which allows for the unbiased interrogation of drugs against the entire, druggable GPCR-ome.

Analgesic studies. Antinociception was assessed using the writhing assay (15) and the radiant heat tail-flick assay (21). The writhing assay assesses the response to an i.p. irritant, either acetic acid or phenylquinone, which yield similar responses. It is a weak stimulus, with activity shown by a wide range of drugs as inactive in thermal assays, such as tail-flick and hot plate. In brief, groups of mice received 1% acetic acid (10 μl/g, i.p.) 15 minutes after receiving the test drug, and writhes were counted from 5–15 minutes after

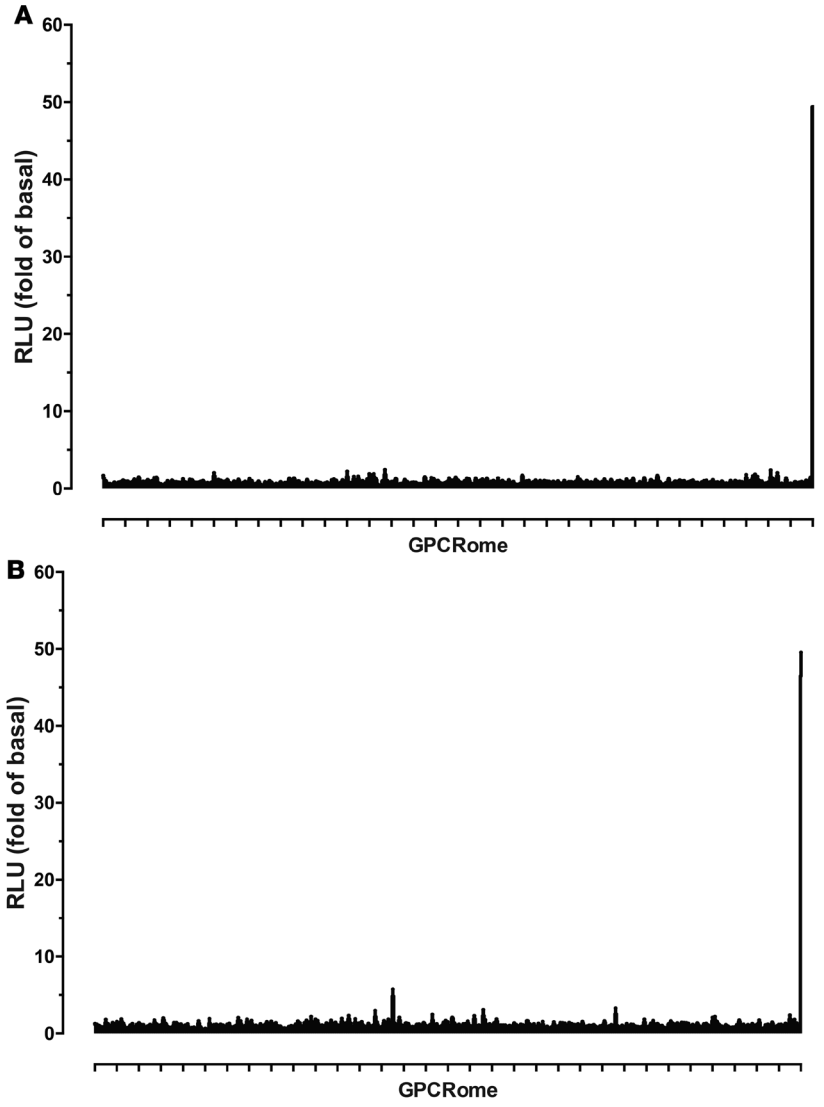

Figure 9. GPCR-ome screening with W-18 and W-15. GPCR-ome screening was conducted according to the PRESTO-Tango assays, as outlined in the Methods. W-15 and W-18 were screened at a final concentration of 1 μM, in quadruplicate for both sample and basal, and results are presented in fold of basal. Dopamine (D_2) receptor with 100 nM quinpirole served as an assay control. **A** represents GPCRome screen of W-18. **B** represents GPCRome screen of W-15.

acetic acid injection The radiant heat tail-flick assay involves placing the tail under a radiant heat source and determining the latency, defined as the time the mouse permits its tail to remain within the light beam. After establishing baseline latencies for each mouse, they receive the test drug and were tested again. A maximal exposure of 10 seconds was used to minimize any tissue damage. Results are provided as percentage maximal effects (%MPE), defined as (test latency – baseline latency)/(10 – baseline latency) × 100.

Predictive pharmacology. We used the similarity ensemble approach (22–24), essentially as previously described (22, 23, 25), to predict potential molecular targets for W-18 and W-15.

Data integrity and reproducibility. All dose-response assays were performed several times and replicated independently, while the GPCR-ome analysis was performed twice in quadruplicate at different concentrations.

Statistics. For the behavioral assays, ANOVA and the 2-tailed Student's *t* test were used with significance predetermined to be at the 0.05 level, thus $P < 0.05$ was considered to be significant.

Study approval. All animal studies were approved by the Institutional Animal Care and Use Committee of Memorial Sloan-Kettering Cancer Center and were conducted in strict accordance with the National Institutes of Health *Guide for the Care and Use of Laboratory Animals* (National Academies Press, 2011) in

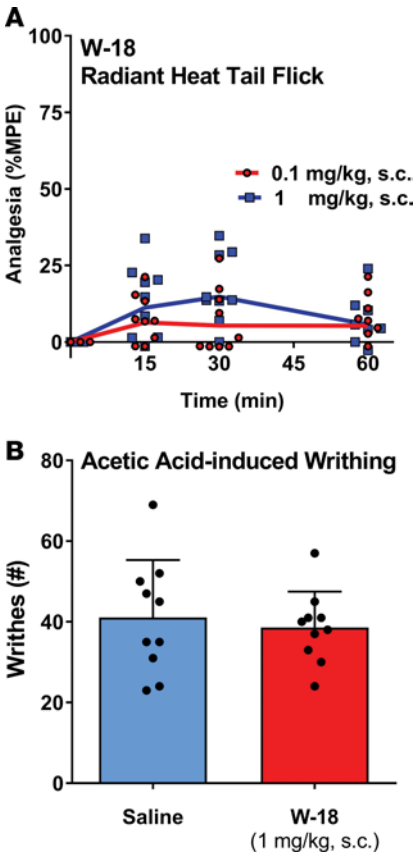

Figure 10. Analgesic activity of W-18 in tail-flick and writhing assays. (**A**) Radiant heat tail-flick: W-18 was tested in the radiant heat tail-flick assay at 0.1 and 1 mg/kg, s.c., as previously described (25). Groups of mice (n = 10) received the indicated dose of W-18, after determining baseline latencies, and were tested at the indicated times. ANOVA revealed no significant differences among groups or times. W-18 (0.1 mg/ml) was dissolved in DMSO (10%), Tween 80 (10%)/water for use at the 1 mg/kg dose. The solution was diluted 10-fold to 0.01 mg/ml for use in the 0.1 mg/kg dose. (**B**) Acetic acid–induced writhing: groups of mice (n = 10) received either saline or W-18 (1 mg/kg, s.c.). Fifteen minutes later, all mice received 1% acetic acid (10 μl/g), and writhes were counted from 5–15 minutes after acetic acid injection. There were no significant differences between the groups by Student's t test.

facilities accredited by the American Association for the Accreditation of Laboratory Animal Care.

Author contributions

GWP was responsible for study design, analysis of behavioral data, and murine receptor characterization and contributed to writing the paper. MHB contributed compounds and assisted with behavioral studies and writing the paper. SM supervised characterization of W-18 in radioligand-binding assays, and MDC supervised the generation of W-18 metabolites and performed metabolite profiling. XPH and TC performed functional assays and analyzed results. TJM performed radioligand-binding assays and analyzed results. BLR was responsible for overall project coordination and writing the paper. VLR and YXP provided chemical synthesis.

Acknowledgments

This work was supported in part by the National Institute of Mental Health Psychoactive Drug Screening Program Contract (HHSN-271-2013-00017-C) and PO1DA035764 from the National Institute of Drug Abuse to BLR, grants from the National Institute on Drug Abuse (DA06241), The MAYDAY Fund, and the Peter F. McManus Charitable Trust to GWP; a core grant from the National Cancer Institute (CA08748) to

Table 3. Behavioral characterization of W-18 in mice

	W-18	Morphine
Analgesia		
Tail flick	Inactive	Active
Acetic acid writhing	Inactive	Active
Hyperlocomotion	Absent	Present
Staub tail	Absent	Present
Burrowing	Present	Absent

Memorial Sloan Kettering Cancer Center; and an equipment grant from the NIH (1S10OD010603) to MDC.

Address correspondence to: Bryan L. Roth, Department of Pharmacology, UNC School of Medicine, 120 Mason Farm Rd., CB # 7365, 4072 Genetic Medicine, Chapel Hill, NC 27599-7365, Chapel Hill, North Carolina 27514, USA. Phone: 919.966.7535; Email: bryan_roth@med.unc.edu.

---

1. Knaus EE, Warren BK, Ondrus TA, inventors; Canadian Patents & Development Ltd., Assignee. Analgesic substituted piperidylidene-2-sulfon(cyan)amide derivatives. US patent 4,468,403. August 28, 1984.
2. Collier HO, Dinneen LC, Johnson CA, Schneider C. The abdominal constriction response and its suppression by analgesic drugs in the mouse. *Br J Pharmacol Chemother*. 1968;32(2):295–310.
3. EMCDDA. European Drug Report 2013: Trends and developments. http://www.emcdda.europa.eu/publications/edr/trends-developments/2013. Accessed November 6, 2017.
4. EMCDDA. European Drug Report 2014: Trends and developments. http://www.emcdda.europa.eu/publications/edr/trends-developments/2014. Accessed November 6, 2017.
5. EMCDDA. European Drug Report 2015: Trends and developments. http://www.emcdda.europa.eu/publications/edr/trends-developments/2015. Accessed November 6, 2017.
6. Gussow L. Toxicology Rounds: Designer Opiates 10,000x Stronger than Morphine. *Emerg Med J*. 2016;38(5):6.
7. Sustkova M. Synthetic Opioids, (re)Emerging Problem in Europe and North America. *Int J Emerg Ment Health*. 2015;17(4):694–695.
8. GONÇALVES J. Order Amending Schedules I and III to the Controlled Drugs and Substances Act (AH-7921, MT-45, W-18 and Lefetamine). Canada Gazette. http://gazette.gc.ca/rp-pr/p1/2016/2016-02-13/html/notice-avis-eng.php-nl3.2016.
9. White KL, et al. Identification of novel functionally selective κ-opioid receptor scaffolds. *Mol Pharmacol*. 2014;85(1):83–90.
10. Wu H, et al. Structure of the human κ-opioid receptor in complex with JDTic. *Nature*. 2012;485(7398):327–332.
11. Vardy E, et al. A New DREADD Facilitates the Multiplexed Chemogenetic Interrogation of Behavior. *Neuron*. 2015;86(4):936–946.
12. Fenalti G, et al. Structural basis for bifunctional peptide recognition at human δ-opioid receptor. *Nat Struct Mol Biol*. 2015;22(3):265–268.
13. Fenalti G, et al. Molecular control of δ-opioid receptor signalling. *Nature*. 2014;506(7487):191–196.
14. Kroeze WK, et al. PRESTO-Tango as an open-source resource for interrogation of the druggable human GPCRome. *Nat Struct Mol Biol*. 2015;22(5):362–369.
15. Spiegel K, Kalb R, Pasternak GW. Analgesic activity of tricyclic antidepressants. *Ann Neurol*. 1983;13(4):462–465.
16. Rothman RB, et al. Evidence for possible involvement of 5-HT(2B) receptors in the cardiac valvulopathy associated with fenfluramine and other serotonergic medications. *Circulation*. 2000;102(23):2836–2841.
17. Roth BL. Drugs and valvular heart disease. *N Engl J Med*. 2007;356(1):6–9.
18. Besnard J, et al. Automated design of ligands to polypharmacological profiles. *Nature*. 2012;492(7428):215–220.
19. Majumdar S, et al. Generation of novel radiolabeled opiates through site-selective iodination. *Bioorg Med Chem Lett*. 2011;21(13):4001–4004.
20. Huang XP, et al. Allosteric ligands for the pharmacologically dark receptors GPR68 and GPR65. *Nature*. 2015;527(7579):477–483.
21. Lu Z, Xu J, Rossi GC, Majumdar S, Pasternak GW, Pan YX. Mediation of opioid analgesia by a truncated 6-transmembrane GPCR. *J Clin Invest*. 2015;125(7):2626–2630.
22. Laggner C, et al. Chemical informatics and target identification in a zebrafish phenotypic screen. *Nat Chem Biol*. 2011;8(2):144–146.
23. Keiser MJ, et al. Predicting new molecular targets for known drugs. *Nature*. 2009;462(7270):175–181.
24. Keiser MJ, Roth BL, Armbruster BN, Ernsberger P, Irwin JJ, Shoichet BK. Relating protein pharmacology by ligand chemistry. *Nat Biotechnol*. 2007;25(2):197–206.
25. Yadav PN, et al. The presynaptic component of the serotonergic system is required for clozapine's efficacy. *Neuropsychopharmacology*. 2011;36(3):638–651.